Mid-infrared reflection signatures for trace chemicals on surfaces

Derek Wood, David B. Kelley, Anish K. Goyal, Petros Kotidis

Derek Wood, David B. Kelley, Anish K. Goyal, Petros Kotidis, "Mid-infrared reflection signatures for trace chemicals on surfaces," Proc. SPIE 10629, Chemical, Biological, Radiological, Nuclear, and Explosives (CBRNE) Sensing XIX, 1062915 (16 May 2018); doi: 10.1117/12.2304453

SPIE.

Event: SPIE Defense + Security, 2018, Orlando, Florida, United States

Mid-Infrared Reflection Signatures for Trace Chemicals on Surfaces[1]

Derek Wood, David B. Kelley, Anish K. Goyal[2], and Petros Kotidis

Block MEMS, 132 Turnpike Road, Southborough, MA 01772

ABSTRACT

Results are presented for the detection of trace explosive residues on real-world surfaces using active mid-infrared (MIR) hyperspectral imaging. The target surface is illuminated using miniature, rapidly tunable, external-cavity quantum cascade lasers (EC-QCLs) and the reflected light is imaged using a HgCdTe camera with a spatial resolution of 70 μm. Hypercubes with 128x128 pixels are captured with more than 256 wavelengths that span 7.7 – 11.8 μm. The samples consisted of PETN residues which were applied to keyboard keys at various levels of chemical loading. We estimate a limit of detection of less than 6 ng per pixel for the as-deposited chemical. The explosive residue remains detectable by HSI even after wiping the surface several times using isopropyl alcohol. Simple signature models for solid particles (i.e., Mie scattering) and thin-films account for the many of the spectral features observed in the chemical signatures.

Keywords: Mid-IR spectroscopy, Quantum cascade laser, Hyperspectral imaging, Chemical detection, HgCdTe focal plane array, Explosives detection

1. INTRODUCTION

Mid-infrared (MIR) spectroscopy is a very promising method for the standoff detection of trace surface chemical because most substances have strong and unique absorption features in the MIR portion of the optical spectrum [1-7]. Our detection approach, active MIR hyperspectral imaging (HSI), involves the use of wavelength-tunable lasers in combination with a high-speed camera to capture hyperspectral images (i.e., hypercubes) of the target surface's reflectance spectrum. These hypercubes are analyzed for spectral features that indicate the presence of the chemicals of interest. A very important application of this technology is the detection of trace explosives.

2. HYPERCUBE ACQUISITION

Our approach to MIR HSI involves the use of external-cavity quantum cascade (EC-QCLs) for laser illumination [5]. Figure 1 shows a photograph of the measurement setup in which the samples were measured at close-range (standoff distance of 8 cm) in order to achieve a high spatial resolution of 70 μm. A composite hypercube with 256 wavelengths was captures across the wavelength range of $\lambda = 7.7 – 11.8$ μm using two of Block's Mini-QCL™ EC-QCLs. The laser beam was raster-scanned across the target to capture an image area of $(8.8\ \text{mm})^2$.

The samples of PETN on black keyboard keys were provided by the Naval Research Laboratory. The PETN was deposited in small localized regions using a dry-transfer technique at chemical loadings ranging from 50 μg to 0.2 μg.

[1] This research was funded by the Office of the Director of National Intelligence (ODNI), Intelligence Advanced Research Projects Activity (IARPA), through the AFRL contract FA8650-16-C-9107. All statements of fact, opinion or conclusions contained herein are those of the authors and should not be construed as representing the official views or policies of IARPA, the ODNI, or the U.S. Government. The Government is authorized to reproduce and distribute reprints for Governmental purposes notwithstanding any copyright annotation thereon.

[2] Corresponding author: anish.goyal@blockeng.com.

Chemical, Biological, Radiological, Nuclear, and Explosives (CBRNE) Sensing XIX, edited by Jason A. Guicheteau, Augustus Way Fountain III, Chris R. Howle, Proc. of SPIE Vol. 10629, 1062915 · © 2018 SPIE · CCC code: 0277-786X/18/$18 · doi: 10.1117/12.2304453

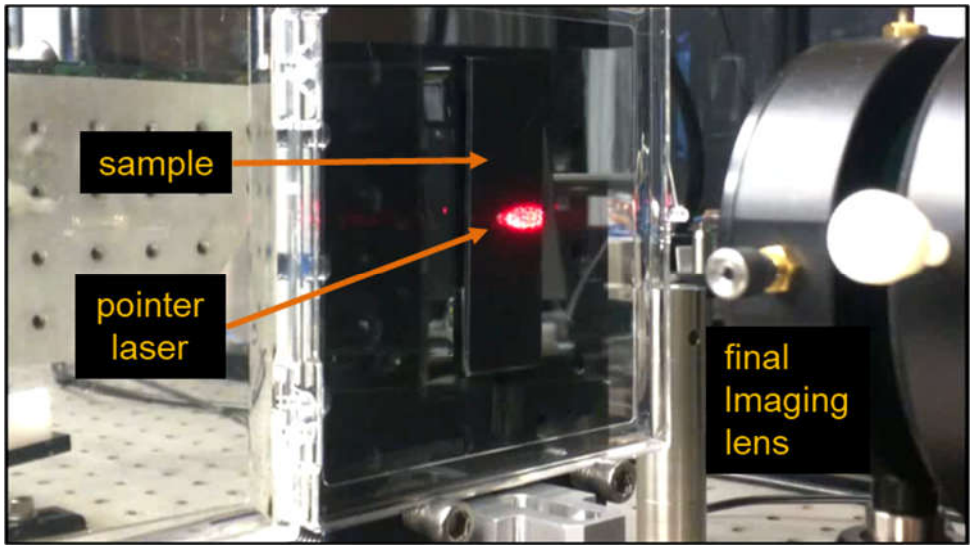

Figure 1. Concept of hyperspectral imaging using a wavelength-tunable MIR laser.

3. RESULTS

Figure 2 illustrates the procedure for creating a detection map for sample with loading of 50 μg of PETN. Shown are a visible image of the sample and frame of the hypercube. The hypercube is analyzed to distinguish areas with clean substrate from the contaminated area. To do so, we compute the variance of the measured spectra at a given pixel with the spectra of its neighboring pixels; if this value is below a certain threshold, the pixel is assumed to contain only clean substrate. These pixels identified as containing clean substrate are shown as red pixels on the detection map in Figure 2.4. The average reflection spectra of each 'clean' pixel is taken to be the best guess for the spectra of the substrate, plotted in red in Figure 2.5.

We next use this data with an adaptive cosine estimation (ACE) algorithm to find pixels contaminated with PETN. Our model for the expected PETN reflectance spectra is calculated with a simple a Mie scattering model, using previously measured complex index of refraction data for PETN as an input. Thresholds are applied to the resulting ACE detection scores to derive the detection map in Figure 2.4 where pixels that were determined to be contaminated with PETN using this method are shown in blue., The average spectra of the contaminated pixels are shown as the blue curve in Figure 2.5, and the average spectra for the clean and contaminated regions starkly shows the difference in reflection spectra. Note also that Figure 2.4 contains regions that are determined to have neither a clean substrate nor a strong enough signal to be considered as containing PETN and are labeled as 'neither.'

Figure 3 shows the results for a sample having a PETN loading of 0.2 μg. Using the analysis procedure described above, the chemical was detected in 33 pixels. Based on this, by assuming each pixel is equally contaminated with the total 0.2 μg, we estimate the detection limit to be about 6 ng/pixel. In fact, we expect the true threshold to be even smaller than this value, because this estimate assumes that the contamination is spread evenly over only these 33 pixels whereas one can see from the visible image that the contamination is more broadly distributed.

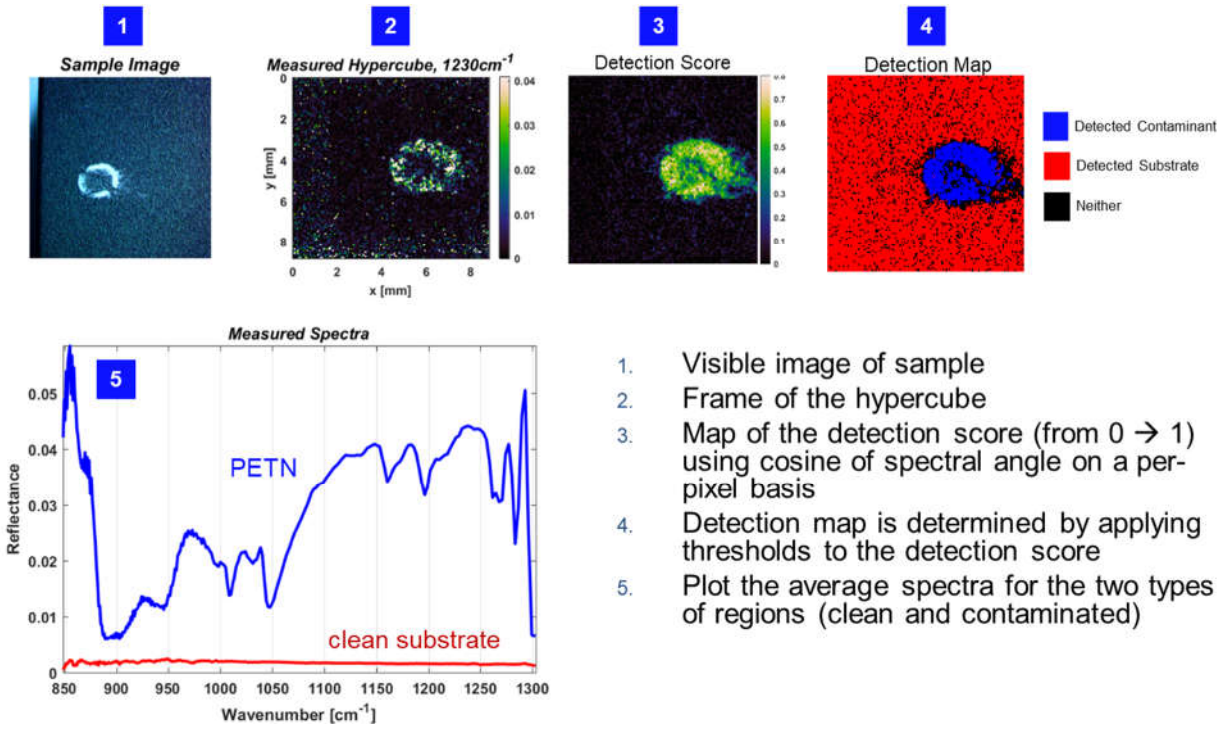

Figure 2. Results for sample with a PETN loading of 50 μg to illustrate procedure for detecting trace residues.

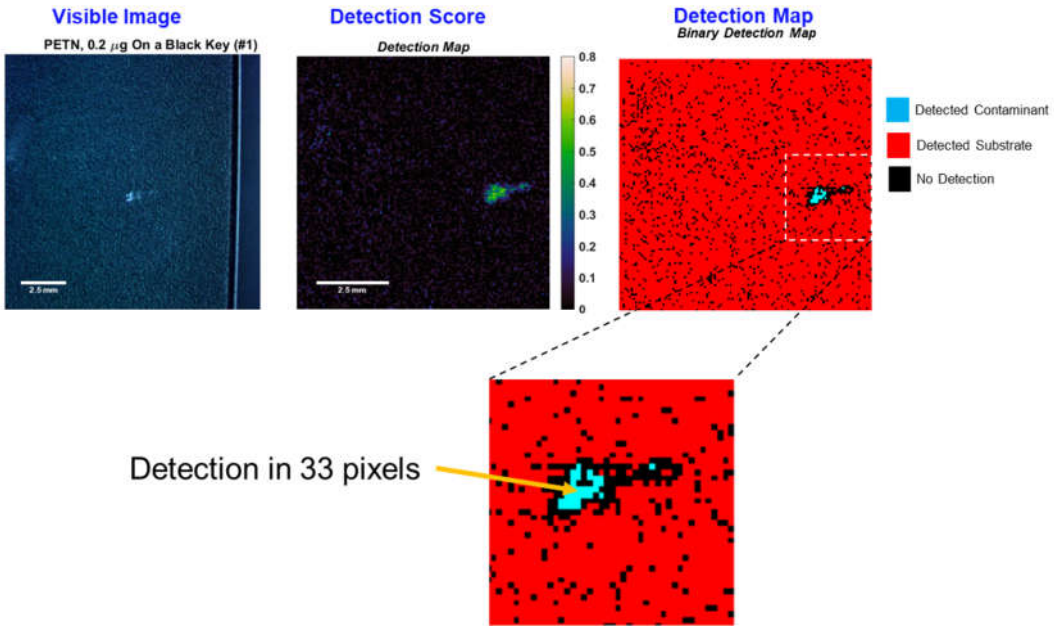

Figure 3. Results for sample with a PETN loading of 0.2 μg.

Figure 4 shows the results for a series of experiments where we wiped the PETN contaminant off of the keyboard key with an isopropanol-soaked cloth. Importantly, even after being wiped away a total of 4 times and leaving no remaining visible evidence of contamination, our attempt at cleaning away the explosive still left behind a prominent and easily identifiable residue. The measured spectra for the PETN detected after being wiped by isopropanol is shown plotted in Figure 5 as the red (wiped 1x) and yellow (wiped 4x) curves. This plot makes clear that the spectral presentation of the PETN contaminant was dramatically changed after being wiped away by the isopropanol cloth (as discussed in greater detail below). Nevertheless, the residual contaminant was still readily identifiable as PETN within the hypercube image.

Figure 5 explains the reason for the observed difference in the pre- and post-wiped PETN reflection spectra. Prior to being wiped away by the isopropanol, the PETN sample had been prepared as a small, localized pile of dry powder, and thus the measured reflection spectra were well modeled by synthetic reflection spectra calculated using a simple Mie scattering model. This model is shown in Figure 5, in the panels to the left; the topmost panel shows the measured spectra for the powdered PETN, the center panel shows the modeled reflection spectra of PETN powder against the measured substrate data, and the bottom panel shows the actual complex component of the index of refraction of PETN. In all three frames, vertical lines have been drawn to highlight similar features in all three plots.

Before discussing the different presentation of the PETN after being wiped away, it is important to first note that PETN is easily dissolved by an isopropanol solvent. The residual PETN left behind after being wiped away is therefore most likely a result of an isopropanol film containing the explosive that evaporated away, leaving behind a thin film of the chemical on the keyboard key. The reflectance spectra of the PETN in this situation is therefore best modeled as a thin film rather than as a sparse powder.

The panels on the right side of Figure 5 demonstrate why this approach is successful. The measured reflectance spectra of the PETN in the top panel is well-matched by the modeled spectra in the center panel, which is found simply by calculating the specular reflection from a smooth surface using the complex index of refraction data for PETN. The same features in the complex index of refraction data are highlighted on the right panels as on the left panels, making it clear that the important features in both spectra are in the same spectral location.

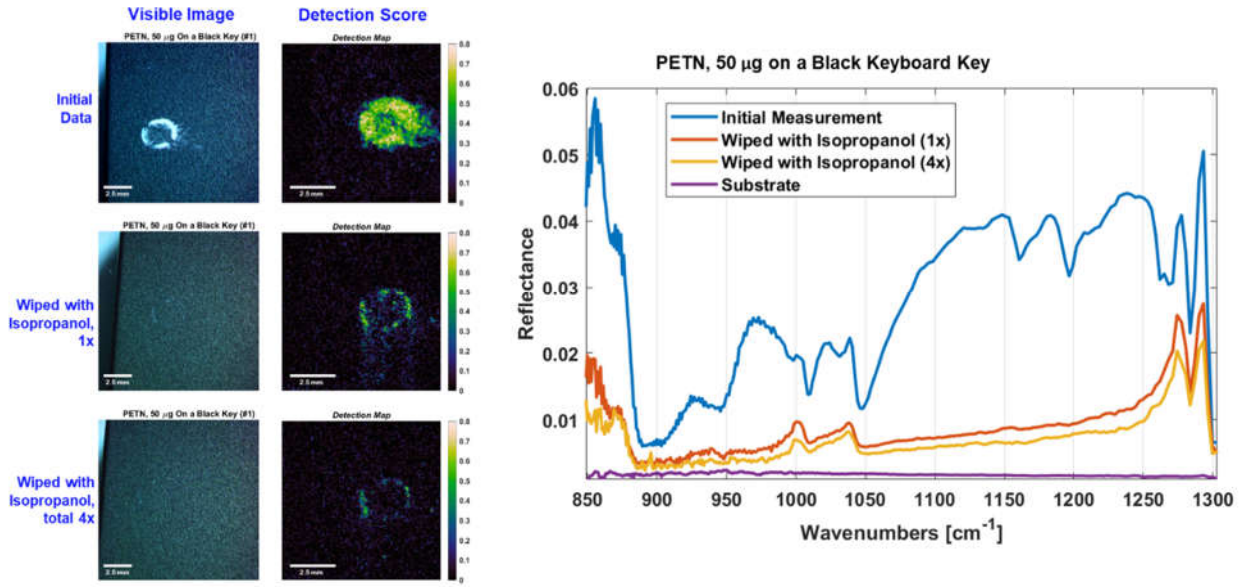

Figure 4. Detection of PETN on keyboard keys both before and after wiping with isopropyl alcohol. After wiping, the shape of the reflection signature changes.

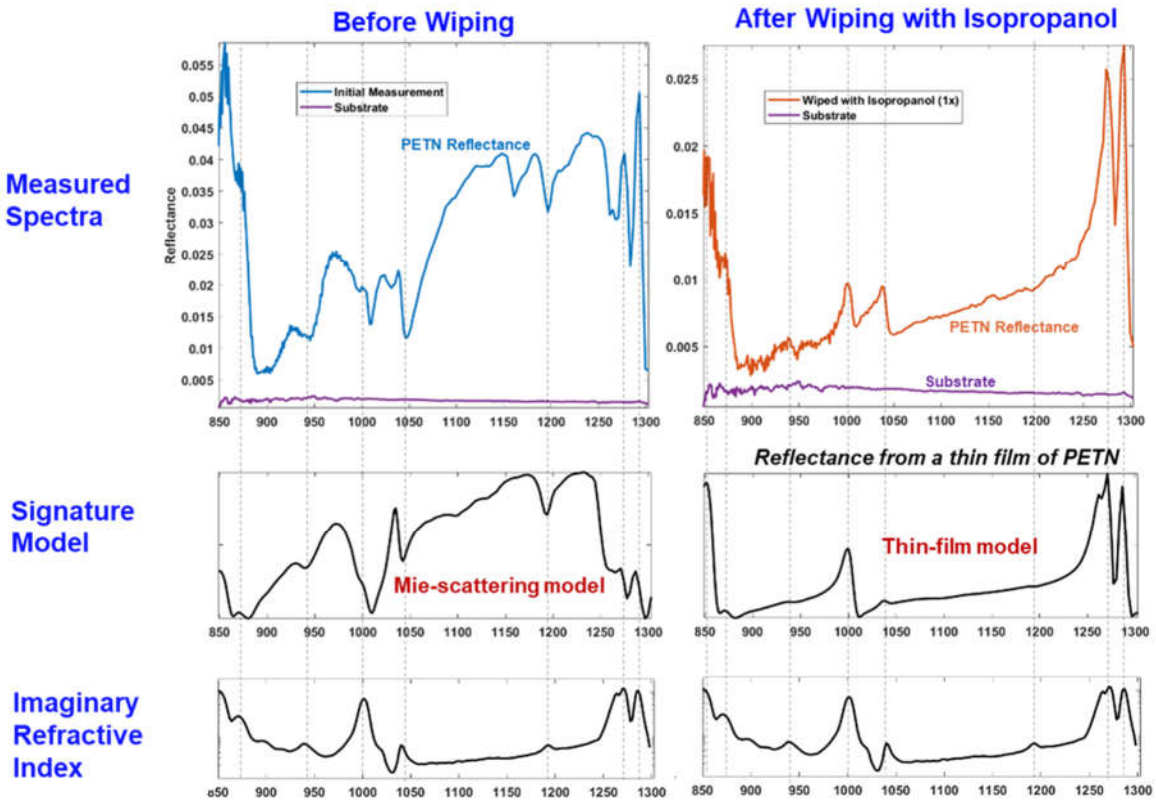

Figure 5. The reflection signature depends on whether the solid is present in the form of solid particles or thin-film. The PETN is observed to appear like a thin-film after wiping with isopropyl alcohol.

4. CONCLUSIONS

We presented results demonstrating the capability of MIR HSI to detect trace levels of explosives on real-world surfaces. For PETN applied to keyboard keys, we obtain a detection limit of better than 6 ng per pixel. The explosive residue remains detectable even after wiping the surface several times using isopropyl alcohol and no visible contamination remains. Simple signature models for solid particles (i.e., Mie scattering) and thin-films account for the many spectral features observed in the chemical signatures.

5. ACKNOWLEDGEMENTS

This work has been supported by the IARPA SILMARILS program through AFRL contract FA8650-16-C-9107. We appreciate the support and expert guidance of the SILMARILS program manager, Dr. Kristin DeWitt. We are grateful to the Naval Research Laboratory (Andy McGill, Chris Kendziora, and Robert Furstenberg) for providing test samples. We also acknowledge numerous interactions with our SILMARILS team members from Alpes Lasers (Richard Maulini) and Systems & Technology Research (Gil Raz, Cara Murphy, Mark Chilenski, and Robert Argo).

REFERENCES

[1] A. K. Goyal and T. R. Myers, "Active mid-infrared reflectometry and hyperspectral imaging", chapter in [Laser-Based Optical Detection of Explosives] CRC Press (2015).
[2] Goyal, A. K., et al., "Active infrared multispectral imaging of chemicals on surfaces," Proc. SPIE 8018, 80180N (2011).
[3] Goyal, A. K., et al., "Active hyperspectral imaging using a quantum cascade laser (QCL) array and digital-pixel focal plane array (DFPA) camera," Opt. Express 22, 14392 (2014).
[4] Ostendorf, R., et al., "Recent Advances and Applications of External Cavity-QCLs towards Hyperspectral Imaging for Standoff Detection and Real-Time Spectroscopic Sensing of Chemicals," Photonics, 3(2), 28 (2016).
[5] Kelley, D. B., et al., "High-speed mid-infrared hyperspectral imaging using quantum cascade lasers," Proc. SPIE 10183, 1018304 (2017).
[6] Myers, T., et al., "Mid-infrared hyperspectral simulator for laser-based detection of trace chemicals on surfaces," Proc. SPIE 10198, 101980C (2017).
[7] Raz, G., et al., "Novel trace chemical detection algorithms: A comparative study," Proc. SPIE 10198, 101980D (2017).
[8] Faist, J. [Quantum Cascade Lasers], Oxford University Press: Oxford, UK, (2013).